PHILOSOPHICAL TRANSACTIONS OF THE ROYAL SOCIETY B BIOLOGICAL SCIENCES

# Characteristic length scales of spatial models in ecology via fluctuation analysis

M. J. Keeling, I. Mezi , R. J. Hendry, J. McGlade and D. A. Rand

*Phil. Trans. R. Soc. Lond. B* 1997 **352**, 1589-1601
doi: 10.1098/rstb.1997.0143

# Characteristic length scales of spatial models in ecology via fluctuation analysis

M. J. KEELING[1,2], I. MEZIĆ[2,3,4], R. J. HENDRY[3], J. MCGLADE[3] AND D. A. RAND[2]

[1] *Zoology Department, University of Cambridge, Cambridge CB2 3EJ, UK* (matt@zoo.cam.ac.uk)
[2] *Nonlinear Systems Laboratory, University of Warwick, Coventry CV4 7AL, UK*
[3] *Ecosystems Analysis and Management Group, University of Warwick, Coventry CV4 7AL, UK*
[4] *Department of Mechanical and Environmental Engineering, University of California, Santa Barbara, CA 93106-5070, USA*

## CONTENTS



## SUMMARY

A technique of fluctuation analysis is introduced for the identification of characteristic length scales in spatial models, with similarities to the recently introduced methods using correlations. The identified length scale provides the optimal size to extract non-trivial large-scale behaviour in such models. The method is demonstrated for three biological models: genetic selection, plant competition and a complex marine system; the first two are coupled map lattices and the last one is a cellular automaton. These cover the three possibilities for asymptotic (long time) dynamics: fixation (the system converges to a fixed point); statistical fixation (the spatial statistics converge to fixed values); and complex statistical structure (the statistics do not converge to fixed values). The technique is shown to have an additional use in the identification of aggregation or dispersal at various scales. The method is rigorously justifiable in the cases when the system under analysis satisfies the FKG (Fortuin–Kasteleyn–Ginibre) property and has a fast decay of correlations. We also discuss the connection between the fluctuation analysis length scale and hydrodynamic limits methods to derive large scale equations for ecological models.

## 1. INTRODUCTION

The importance of spatial models in ecological systems has become clear over the last few years. Whilst many studies have used continuous systems (such as reaction–diffusion equations) or implicit spatial systems (patch models), discrete models are becoming increasingly popular for modelling biological populations. Reviews of these alternative types of spatial models include Czárán & Bartha (1992) and Durrett & Levin (1994*a*). Discrete biological models have primarily been probabilistic cellular automata or in-

teracting particle systems (Weiner & Conte 1981; DeRoos *et al.* 1991 and Levin & Durrett 1996). In contrast to cellular automata, which take discrete values on a discrete grid, coupled map lattices deal with continuous variables; examples of biological applications of these models include Hassell *et al.* (1991) and Solé & Valls (1991).

An important problem in biological modelling and data collection, highlighted by the use of spatial models, is that of the establishment of length scales. It is well known that in spatially extended systems many different spatial scales can be important. For example, there are interactions between neighbouring individuals and there are dynamics on population, community and ecosystem scales. Therefore, an important issue in the study of mathematical or computational spatial models is the identification of spatial scales intrinsic to the system. The use of a discrete lattice introduces three imposed length scales. The cell size is the smallest of these length scales and may be related to the size, or area of direct influence of a sessile organism, or the space covered by a motile individual in a fixed interval of time. The size of the neighbourhood, usually defined in terms of the cell size, is the range over which biological interactions occur. The largest imposed scale is the length of the system ($L$), which gives the total number of cells as $L^d$ (where $d$ is the dimension of the spatial model, usually $d = 2$). All of the above are *a priori* length scales, set up as the assumptions of a model. An important *a posteriori* length scale would be the emergent scale at which the dynamics progress. This has usually been approximated by the *classical correlation length*. The classical correlation length is the separation distance $D$ such that the correlations between two sites at distance $r$ decays as $\mathrm{e}^{-r/D}$ for large $r$. Unfortunately this is difficult to measure and often a definite answer cannot be obtained.

In this paper the *coherence length scale* ($\ell_c$) is introduced and analysed. This length scale corresponds (in the way described below) to the one introduced by Rand & Wilson (1995). For 'windows' of a much smaller size than $\ell_c$ there are strong correlations between the individual sites, while disjoint windows of a much larger size are statistically independent. It is desirable to average the data over the boxes of the size of the coherence length $\ell_c$. If the data is averaged over smaller boxes the observed non-trivial dynamics may be too complicated, and if the data is averaged over larger boxes any non-trivial dynamics will be averaged out. It should be pointed out that, in order to *rigorously justify* the method that we use, we need a sufficiently fast (e.g. exponential) decay of correlations; so, from the mathematical point of view, one is not completely freed from analysing the decay of correlations using this approach. On the other hand, using the method developed here numerically, $\ell_c$ is typically easily determined, and the prescription that we give does not involve calculating the correlation length. Throughout this work we are assuming that the system size ($L$) is sufficiently larger than the size of the window ($\ell_c$) so that boundary effects are negligible. Actually in all simulations shown here the system size is always greater than twice the largest averaging window size.

The length scale problem has been addressed by a few authors, such as Wiens (1989), DeRoos *et al.* (1991), Wissel (1991), Levin (1992), Rand & Wilson (1995) and Rand (1994). This paper presents a method for determining the coherence length scale of spatially extended models, using the analysis of fluctuations at varying scales. The method is applied to three examples, of which one is a probabilistic cellular automaton, one is a coupled map lattice and one is a hybrid between a probabilistic cellular automaton and a coupled map lattice; this technique has also been successfully applied to other systems (Rand *et al.* 1995; Hendry & McGlade 1995; Keeling & Rand 1996; Keeling 1997). All of the models use toroidal grids (periodic boundary conditions), space discretized into square cells and synchronous updating, although these conditions are not essential for the method described: in fact asynchronous updating allows the formulation of many analytical results on spatially extended models (see Liggett 1985). These examples demonstrate different types of behaviour. The first model is the simplest: every tested initial condition approaches an invariant equilibrium configuration at long times, although the configuration depends on the initial conditions. We call this type of model *system with fixation*. The second model displays asymptotic statistical structure that is constant in time (i.e. the invariant measure to which the system converges is ergodic, see Appendix 1), and we call it a *system with statistical fixation*. The final example shows more complex asymptotic statistics and the invariant measure to which the system converges is not ergodic. These descriptions are based on our numerical simulations. Unfortunately, none of them can be justified rigorously for the systems we study, due to their complexity.

The next section presents the theory and numerical treatment for systems with fixation and statistical fixation, before extending the ideas to models with complex statistics. This brings out one of the main differences between our study and the previous work of Rand & Wilson: for stationary and statistically stationary systems the two approaches are similar—the length scale is calculated using the global average density $\mu$. But, for systems that exhibit non-trivial dynamics of average quantities at some scale, we use the theory of nonlinear prediction (see Casdagli 1989). The theory consists of a semi-heuristic approach based on treating neighbouring sites as independent random variables, and a more rigorous treatment, using the FKG (Fortuin–Kasteleyn–Ginibre) property that some coupled map lattices and probabilistic cellular automata possess (see Mezić 1997). In particular, we show that our genetic selection model possesses the FKG property. In § 3 the models are introduced. The results of the application of the coherence length scale technique are presented and discussed in § 4. In § 5 we provide a connection between the length scale, $\ell_c$, and modelling. This connection arises by observing that this

length scale determines the size of almost independent windows, and linking this to the hydrodynamic analysis of the type used by Durrett & Levin (1994*b*). For this purpose, we perform fluctuation analysis on the same system that Durrett & Levin used in their study: the spatially extended hawk–dove game. The paper ends with the discussion of results in § 6, and three mathematical appendices.

## 2. THE FLUCTUATION ANALYSIS METHOD

### (*a*) *Systems with fixation and statistical fixation*

Let us first introduce the definitions for fixation and statistical fixation. Fixation means that, asymptotically in time, the system approaches a fixed point. Different spatial structures of the asymptotic configuration can be achieved by starting from different initial conditions. Statistical fixation means that, after transients, the system moves randomly through different configurations, but each of these configurations has statistically the same spatial structure. A more precise definition is that, asymptotically in time, the distribution of a system converges to an invariant ergodic measure (see Appendix 1).

The identification of the coherence length scale, $\ell_c$, can be approached by analysing the fluctuations arising at different spatial scales. Our models are defined on the lattice $\boldsymbol{Z}^2$, but all the theoretical considerations are valid for systems on $\boldsymbol{Z}^d$, as well. To each site $i \in \boldsymbol{Z}^d$ we can assign a number $x_i = V(i)$ that denotes the state of the system at that site. $V$ is a function $V : \boldsymbol{Z}^d \to \boldsymbol{R}$ or $V : \boldsymbol{Z}^d \to \boldsymbol{Z}$. We are going to call $\boldsymbol{x} = \{x_i, i \in \boldsymbol{Z}^d\}$ a *configuration*.

For any configuration $\xi$ the spatial average $A_\ell(\xi)$, on a window of size $\ell^d$, is

$$A_\ell(\xi) = \frac{1}{\ell^d} \sum_{i \in W_\ell} x_i.$$

Consider the long-term time average of $A_L$,

$$\mu = \lim_{T \to \infty} \frac{1}{T} \sum_{t=t_0}^{t_0+T} A_L(\xi(t)) = \langle A_L \rangle_t,$$

where $L$ is the system size, and angled brackets denote long term averages. Assuming ergodicity of the process,

$$\mu \equiv \sum_{\xi} A_L(\xi)\nu(\xi),$$

where $\nu$ is the invariant measure of the system (see Liggett 1985). Note that the ergodicity of the system does not necessarily mean the ergodicity of its invariant measure, as explained in Appendix 1. In the case of systems with more than one asymptotic limit (which depends on initial conditions), we either need to perform an average over all initial conditions, or else treat the different basins of attraction of the measure separately.

We analyse the fluctuations of $A_\ell$ about $\mu$ for various window sizes $\ell$ by investigating the scaling of the standard deviation $E_\ell$,

$$E_\ell = \langle [A_\ell(\xi(t)) - \mu]^2 \rangle_t^{1/2}.$$

When $\ell$ is such that the windows are independent, it is reasonable to ask if the central limit theorem applies. In that case $E_\ell$ should scale as $\sqrt{1/\ell^d}$ when $\ell$ is large enough. In applications we will check if this is true by plotting a graph of

$$X_\ell = \sqrt{\ell^d} E_\ell,$$

against $\ell$. We call this graph a *fluctuation diagram*. The *coherence length scale*, $\ell_c$, is defined to be the point where $X_\ell$ asymptotes to a constant value (see figures 2, 4, 7 and 8). Let us now consider how the change of $X_\ell$ can be interpreted in terms of the spatial structure. We shall show that increases in $X_\ell$ correspond to aggregation and decreases to disaggregation.

If we assume

$$X_{\ell+1}^2 > X_\ell^2,$$

$$\text{then} \quad \frac{1}{(\ell+1)^d} \operatorname{var}(S_{\ell+1}) > \frac{1}{\ell^d} \operatorname{var}(S_\ell).$$

Note that the variance in the sum over a window ($S_\ell = \ell^d A_\ell$) can be decomposed into the variance at each point and the covariance between points,

$$\operatorname{var}(S_\ell) = \sum_{i \in W_\ell} \operatorname{var}(x_i) + \Big\langle \sum_{\substack{i \neq j \\ i,j \in W_\ell}} x_i x_j \Big\rangle.$$

Because we assume spatial homogeneity $v = \operatorname{var}(x_i)$ is independent of $i$, we can deduce:

$$\frac{1}{(\ell+1)^d} \left[ (\ell+1)^d v + \Big\langle \sum_{\substack{i \neq j \\ i,j \in W_{\ell+1}}} x_i x_j \Big\rangle \right]$$

$$> \frac{1}{\ell^d} \left[ \ell^d v + \Big\langle \sum_{\substack{i \neq j \\ i,j \in W_\ell}} x_i x_j \Big\rangle \right]$$

$$\Longrightarrow \frac{1}{(\ell+1)^d} \sum_{i \in W_{\ell+1}} \operatorname{cov}(x_i, S_{\ell+1} - x_i)$$

$$> \frac{1}{\ell^d} \sum_{i \in W_\ell} \operatorname{cov}(x_i, S_\ell - x_i).$$

This implies that when $X_\ell$ is increasing the average covariance between a site and the rest of the window (a measure of aggregation) also increases with window size; the converse also holds. Thus if $X_\ell > X_1$ the sites are aggregated at this scale as the value of the window lies further from the mean, on average, than a distribution of sites using the invariant measure $\nu$ predicts.

It is interesting to discuss these results in terms of renormalization theory. In particular, the change of $X_\ell$ as we increase $\ell$ gives us some indication of how the system changes if we look at it at larger and larger scales. A typical example of a fluctuation diagram shows $X_\ell$ increasing with $\ell$ and then asymptoting to some constant value (see figure 2). This constant value indicates how much variance is left in the renormalized state of the system, where each big

window of size $\ell$ is one site. For very large $\ell$ the system is completely uncorrelated, i.e. the neighbouring windows are independent, and $\lim_{\ell\to\infty} X_\ell = c$. For a system in which the neighbouring sites are completely independent, $X_\ell$ is a constant which does not depend on $\ell$. But for a system that looks the same at all scales, this should also be true. Thus we expect the fluctuation analysis to suggest the cases in which the asymptotic state of the system has a self-similar structure on all scales. It is necessary to point out that this vague criterion is based only on analysing the second moment of the renormalized distribution, and for a proper proof of self-similarity one would have to consider how the whole distribution changes as we increase the length scale (see, for example, Sinai 1976). But one is typically faced with unsurmountable technical problems when trying to establish the self-similarity for complicated multispecies systems. In this sense the above heuristic discussion can be useful.

### (*b*) *Systems with complex statistics*

We now consider systems in which the behaviour of the averaged quantities in the finite window cannot be described as random fluctuations around a global average. As we increase the size of the averaging window, such a system asymptotes to a state in which independent windows exhibit non-trivial dynamics—dynamics which are *not* just fluctuations around the global average, but have a non-trivial deterministic component to them. As we increase the size of the measurement window even more, we start averaging over different, almost independent, dynamics. As these dynamics are not in phase, we get closer and closer to some global average, $\mu$. In short, globally the system exhibits average values constant in time, while on some intermediate scale, $\ell_c$, the average values show non-trivial deterministic behaviour.

When dealing with this more complex behaviour, Rand & Wilson (1995) have proposed to consider the deviation from the infinite system average, $\mu$, to identify the scale at which the dynamics occur, as done for the stationary and statistically stationary systems in the previous sections of this paper. We propose that an improvement in the identification of the intermediate scale, $\ell_c$, can be obtained when we consider the details of the deterministic dynamics in the window. We assume that the dynamics in the window of the size $\ell_c$ can be approximated by the deterministic rule

$$\mu(t+\tau) = F(\mu(t), \mu(t-\tau), \ldots, \mu(t-n\tau)), \qquad (1)$$

for some integer, $n$. For the systems treated in the previous section $\mu(t) = \mu$. We consider the fluctuation

$$E_\ell = \langle [A_\ell(\boldsymbol{x}(t)) - \mu(t)]^2 \rangle_t^{1/2},$$

and check if it starts scaling as $\sqrt{1/\ell^d}$ at the length scale $\ell_c$, in accordance with the central limit theorem.

In the practical implementation of the method described above, we use prediction algorithms for time series as our function $F$ (see Casdagli 1989). This prediction may require the values of several previous states and so we define

$$\boldsymbol{B}_\ell(\boldsymbol{x}(t)) = (A_\ell(\boldsymbol{x}(t)), A_\ell(\boldsymbol{x}(t-\tau)), \ldots, A_\ell(\boldsymbol{x}(t-n\tau))).$$

For each window size, assuming the dynamics have underlying determinism, it is possible to calculate a predictor function, $\tilde{F}_\ell$ using one of the standard techniques, for example radial basis functions (Casdagli 1989) or by comparison to past values.

$$\tilde{F}_\ell(\boldsymbol{B}_\ell(\boldsymbol{x}(t-\tau))) \approx A_\ell(\boldsymbol{x}(t)).$$

The accuracy of the predicting function will increase with the size of the learning set (the set of $\boldsymbol{B}$ values used to calculate the function), and as this becomes large the fluctuation will tend to the previous form.

$$E_\ell = \langle [A_\ell(\boldsymbol{x}(t)) - \tilde{F}_\ell(\boldsymbol{B}_\ell(\boldsymbol{x}(t-\tau)))]^2 \rangle_t^{1/2} \propto \sqrt{1/\ell^d}.$$

The remainder of the calculation follows as before, finding the characteristic length scale by comparing $X_\ell$ with $\ell$. The assumption that there is an underlying deterministic system at the coherence length scale $\ell_c$ can be checked by comparing $E_{\ell_c}$ with

$$E'_{\ell_c} = \langle \langle [A_{\ell_c}(\boldsymbol{x}(t_1)) - \tilde{F}_{\ell_c}(\boldsymbol{B}_{\ell_c}(\boldsymbol{x}(t_2-\tau)))]^2 \rangle_{t_1} \rangle_{t_2}^{1/2},$$

which is the average distance between all predicted points and all actual points. If $E_{\ell_c} \ll E'_{\ell_c}$ then the dynamics closely follow the orbit predicted by $\tilde{F}$, otherwise either all the fluctuations over the window are due to noise or the method of prediction has insufficient accuracy.

As pointed out above, this result is related to the length scale proposed by Rand & Wilson (1995), with the exception that the reference average in the fluctuation analysis done by these authors is the global average, and the averaging is performed over a finite time interval. Averaging for finite time $T$ in our case, we obtain a result similar to Rand & Wilson (1995):

$$E_\ell = \langle [A_\ell(\boldsymbol{x}(t)) - F_\ell(\boldsymbol{B}_\ell(\boldsymbol{x}(t-\tau)))]^2 \rangle_t^{1/2} \propto c_0(T) + \sqrt{1/\ell^d},$$

where $c_0(T) \to 0$ as $T \to \infty$, if the deterministic dynamics are chaotic.

### (*c*) *Systems with FKG property*

Note that the above derivations rely essentially on the fact that the analysed systems satisfy the conditions for the central limit theorem to hold. The central limit theorem would hold if we could treat the value at each site as an independent random variable. But this is typically not true. What is true, most commonly, is that the correlations between sites decay exponentially fast; however, there are very simple models that are exceptions, e.g. the voter model in one dimension, described for example in Liggett (1985). If the correlations decay sufficiently fast, so that

$$\sum_{k\in\boldsymbol{Z}^d} \mathrm{cov}(x_0, x_k) < \infty,$$

$$p'_{ij} = \frac{\alpha p_{i,j}\Sigma_{i,j} + \frac{1}{2}\beta p_{i,j}(1-\Sigma_{i,j}) + \frac{1}{2}\beta(1-p_{i,j})\Sigma_{i,j}}{\alpha p_{i,j}\Sigma_{i,j} + \frac{1}{2}\beta p_{i,j}(1-\Sigma_{i,j}) + \frac{1}{2}\beta(1-p_{i,j})\Sigma_{i,j} + \gamma(1-p_{i,j})(1-\Sigma_{i,j})}, \quad (2)$$

and the system has the so-called FKG property, Newman (1980) has shown that the central limit theorem is satisfied. In that case the discussion above becomes rigorous. The FKG property and its relevance to the length scale problem is examined in Appendix 2. The FKG inequalities (or the preservation of those) are typically easy to verify analytically for the types of systems that we study here. It is the decay of correlations and the convergence to an invariant measure that is typically hard to prove.

## 3. THE MODELS

### (a) *Genetic model with heterozygote inferiority: a system with fixation*

This model examines selection at a single diallelic locus in a spatially extended population. The alleles are labelled **a** and **A** and their fitness is fixed with heterozygote inferiority. The population exists on a two-dimensional square lattice and we denote the proportion of alleles **a** in cell $(i, j)$ by $p_{ij}$. If the members of each cell are allowed to mate randomly within the cell and also with the four nearest neighbours, then at the next generation $p'_{ij}$ is given by equation (2) above.

In equation (2)

$$\Sigma_{ij} = \frac{1}{5}\sum_{(k,l)\in \mathrm{Nhd}(i,j)} p_{kl}.$$

Nhd is the five-cell von Neumann neighbourhood and $\alpha$, $\beta$ and $\gamma$ are, respectively, the fitnesses of **aa**, **aA** and **AA**. This model is the spatial equivalent of standard simple genetic competition models with coupling between local sites. Equation (2) is simplified by dividing through by $\beta$ and setting

$$A = \frac{\alpha-\beta}{\beta}, \quad B = \frac{\gamma-\beta}{\beta}.$$

The condition $A = B$ means that both homozygote genotypes have equal fitness, and so the system is symmetric with respect to switching **a** and **A**.

### (b) *Plant competition model: a system with statistical fixation*

Competition between annual and perennial plants is modelled using a two-dimensional coupled map lattice. Only a single plant may grow in each site of the lattice and the variable $m_{i,j}$ records the plant mass. The model is described in detail in Hendry *et al.* (1996), but can be summarized as follows. Within season growth is given by

$$\frac{\mathrm{d}m_{i,j}}{\mathrm{d}t} = g(a_{i,j} - l_{i,j}) - bm_{i,j}^2$$

$$a_{i,j} = cm_{i,j}^{2/3}.$$

$g$ is the intrinsic growth rate, $a_{i,j}$ is the space required by the plant at $(i, j)$, $l_{i,j}$ is the space lost to competing neighbours and $b$ and $c$ are constants. The second equation describes the self-thinning rule. Competition is asymmetric, so that a disputed area where two plants overlap goes to the larger plant. As in the previous model the neighbourhood is the five-cell (von Neumann) type.

The behaviour of the plants at the end of each year is based on the cellular automaton model of Crawley & May (1987). At the end of the growing season all of the annual plants produce seeds, in numbers proportional to their sizes, and die. The seeds are distributed normally so that the the expected displacement from the parent plant is

$$\frac{\sqrt{2}P_\mathrm{s}}{(P_\mathrm{s}-1)^2}.$$

This is an increasing function of $P_\mathrm{s}$, and for $P_\mathrm{s} = 1$ the seeds are randomly scattered over the whole grid. The perennials propagate vegetatively by ramets depending on the total mass in the four neighbouring cells. At the end of each year there is a small probability of perennial death. The perennial ramets are assumed to have complete competitive advantage over the annual seedlings at the reproduction stage (i.e. seeds from annuals are only able to grow in any cells that remain uncolonized). Thus the surviving perennials, new perennial ramets and the new annual seedlings together contribute to the initial conditions for the following year's growth, controlled by the given differential equation.

For this system measurements are made at the end of each growing season, recording the mass and type of each plant.

### (c) *Multispecies marine ecosystem: a system with complex statistics*

This model is an artificial ecology (Rand & Wilson 1995) where sea otters and urchins move over a background of kelp and microalgae. The otter searches for urchins which are a key food source; if it has recently fed (within the last five iterations), an otter may breed, but if it has been deprived of food for too long (over 30 iterations) it dies.

The urchins can eat either kelp or microalgae, but will only resort to eating algae when there has been no kelp available for nine iterations. Reproduction and death of urchins again depends upon when food was last consumed (reproduction only occurring within two iterations and death after 10 iterations since the last meal).

Both algae and kelp grow over bare substrate, but the algae does so far faster; the probabilities for colonizing an adjacent site are 0.2 and 0.01, respectively. Kelp however can invade areas covered by algae more rapidly than areas of bare substrate (with probability

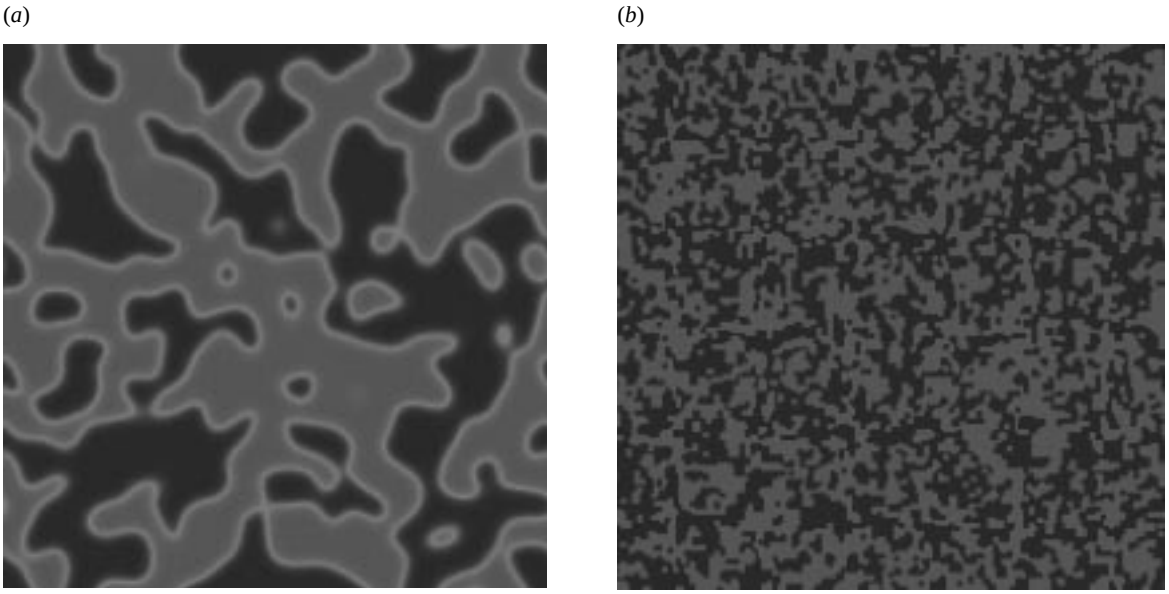


Figure 1. An example of the final state spatial pattern from a 200×200 lattice of the genetic model with (*a*) $A = B = 0.1$ and (*b*) $A = B = 100$.

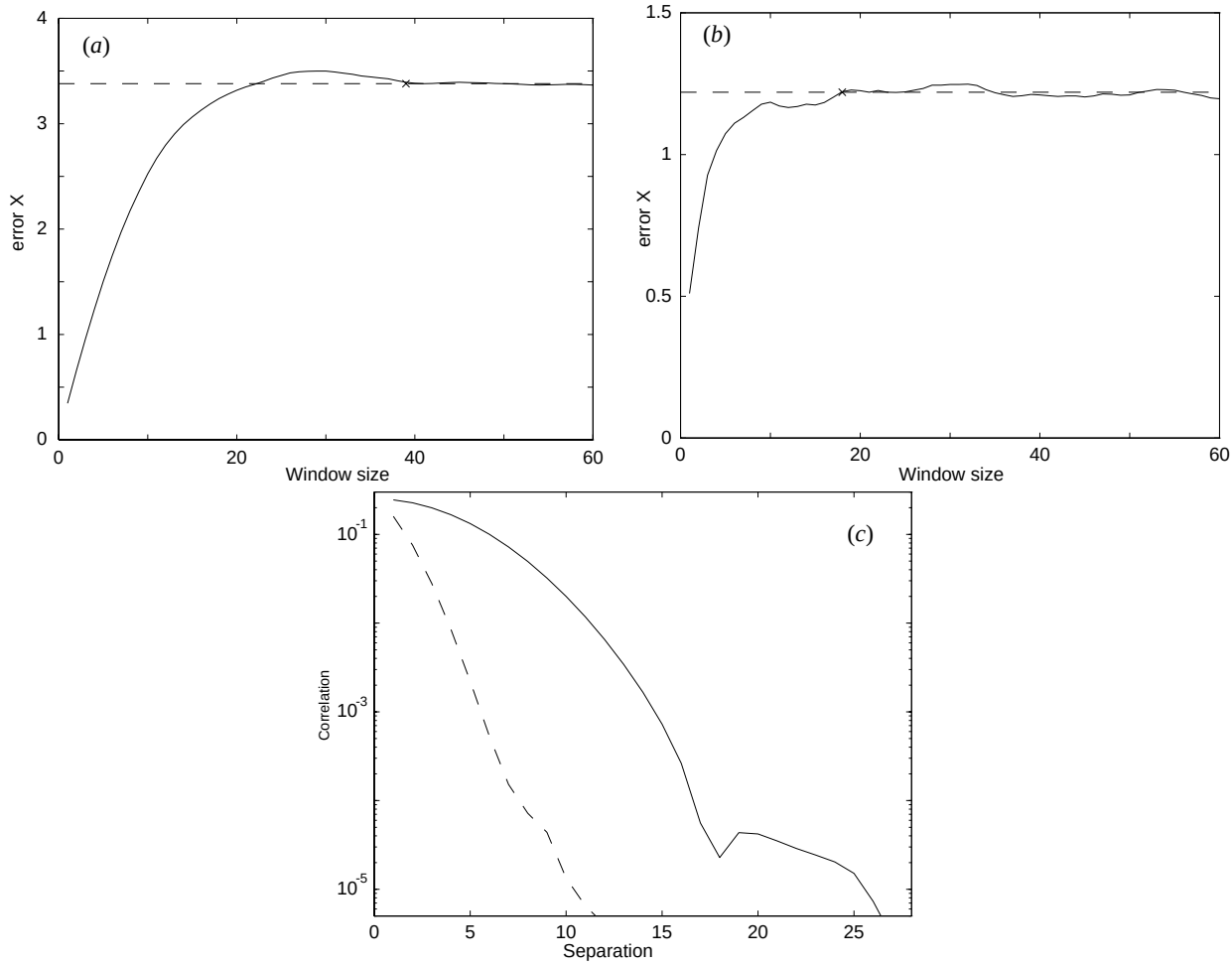


Figure 2. Fluctuation diagrams for the genetic model: (*a*) $A = B = 0.1$ and (*b*) $A = B = 100$. (*c*) The correlations decay exponentially fast for both sets of parameters. The solid line is for $A = B = 0.1$, the dashed line $A = B = 100$.

0.05). Predation occurs when two creatures occupy the same site; movement and growth are to the nearest four cells although otters can 'sense' urchins from a distance of two cells and move towards them.

In general the system can be summarized as follows, algae is a good colonizer but kelp is a better competitor, although large beds of kelp are more readily consumed by urchins, which in turn fall prey

to otters. It is this existence of multiple feed backs that lead to the complex dynamics of this system. This model is discussed in more detail in McGlade (1995).

## 4. RESULTS AND DISCUSSION

### (a) *Genetic model with heterozygote inferiority: a system with fixation*

The numerical simulations show that this system tends to a fixed spatial pattern, which is highly dependent on the initial conditions. The transients are fairly rapid and after only 200 iterations convergence to the attractor has been achieved. The system was always started with uniformly distributed random initial conditions; however, if the initial conditions are biased or if $A \neq B$ then the size of the patches is similarly biased, or in extreme cases one allele may become extinct.

When the general spatial pattern of the system is examined for two widely different values ($A = B = 0.1$ and $A = B = 100$), it is seen that smaller parameter values give rise to larger structures and therefore a larger length scale (figure 1). When $A = B = 0.1$ there is only a slight advantage in being homozygote, and as might be expected the homogeneous patches are large and the boundaries between the regions are wide and diffuse. When $A$ and $B$ are increased to 100 there is a huge selective pressure towards being homozygote hence the boundaries become smaller (of the order of one site) and sharper. This in turn leads to smaller patches being stable so that the length scale is smaller. Although this qualitative result is immediate from observation, a more quantitative answer can be found using our technique. As this is an equilibrium system, $E_\ell$ was averaged over several hundred simulations (as opposed to iterations) for improved numerical accuracy. Plotting $X_\ell$ against $\ell$ (figure 2) the coherence length is easily identified. For $A = B = 0.1$, the length scale is about $40 \times 40$ cells, whereas for $A = B = 100$ the scale has decreased to about $18 \times 18$ cells. The fluctuation diagram shows an increase in $X_\ell$ before it settles to a constant, which indicates an increase in aggregation until $\ell_c$, with the larger patches and therefore more aggregated distribution of the first simulation producing higher values of $X_\ell$.

It can be checked that this coupled map lattice satisfies the conditions for FKG when $A = B$ (see Appendix 3) and we have shown numerically that the correlation between two sites decays exponentially with their separation (figure 2*c*). Together these two conditions are all that is necessary for the central limit theorem to hold, hence our assumption that $X_\ell$ tends to a constant is justified.

### (b) *Plant competition model: a system with statistical fixation*

Figure 3 shows a typical plant distribution after 100 years for a $100 \times 100$ grid, for the case where

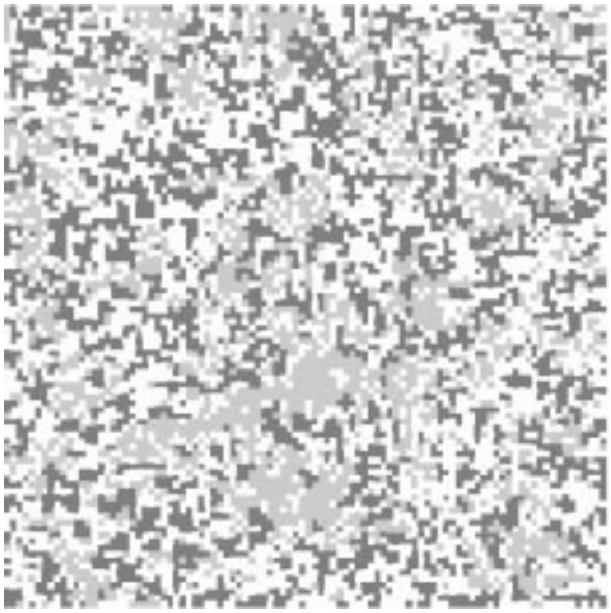

Figure 3. Example of the plant competition model: spatial pattern of a mixed population after 100 years. Dark cells are perennials, grey cells are annuals and light cells are empty.

perennial mortality is zero and $P_s = 0.7$. The fluctuation analysis was carried out over a 50 yr period, allowing 50 yr for transient behaviour. Plotting fluctuation diagrams for two values of $P_s$ and separate communities of annuals and perennials (figure 4), it is clear that the asymptotic fit is not as close as in the previous example as the sample size is much smaller, and there are strong stochastic elements present in each season.

For figure 4*a*, $P_s = 0.7$ and hence the seeds tend to be scattered over a fairly large distance, approximately 11 cells. For figure 4*b* $P_s$ has been reduced to 0.3 and this in turn reduces the scattering distance to less than one cell. Both simulations display a similar coherence length scale of approximately 130, but whereas for the genetic model $X_\ell$ was monotonic, for this system the behaviour is more complex. There is strong aggregation for windows of less than 100 cells, but above 130 cells $X_\ell$ returns close to the value of $X_1$. This means that we should observe large patchy behaviour in windows of around 50–100 cells but at larger sizes there is a regularity about the distribution of patches which reduces $X_\ell$. It can be seen that in figure 4*a* the greater dispersal of the annuals leads to a more even distribution of this species which in turn produces smaller fluctuations than are observed in figure 4*b*.

Figures 4*c*, *d* are for communities composed solely of annuals and perennials, respectively. Perennials are less aggregated than annuals at the larger scales. Perennials propagate by ramets and due to this localized spread are subject to intense intraspecific competition. This leads to very little aggregation with disaggregation predominating at lengths above 40 cells. Annuals on the other hand spread over a larger area experiencing less competition and therefore demonstrating higher levels of aggregation.




PHILOSOPHICAL TRANSACTIONS OF THE ROYAL SOCIETY B BIOLOGICAL SCIENCES

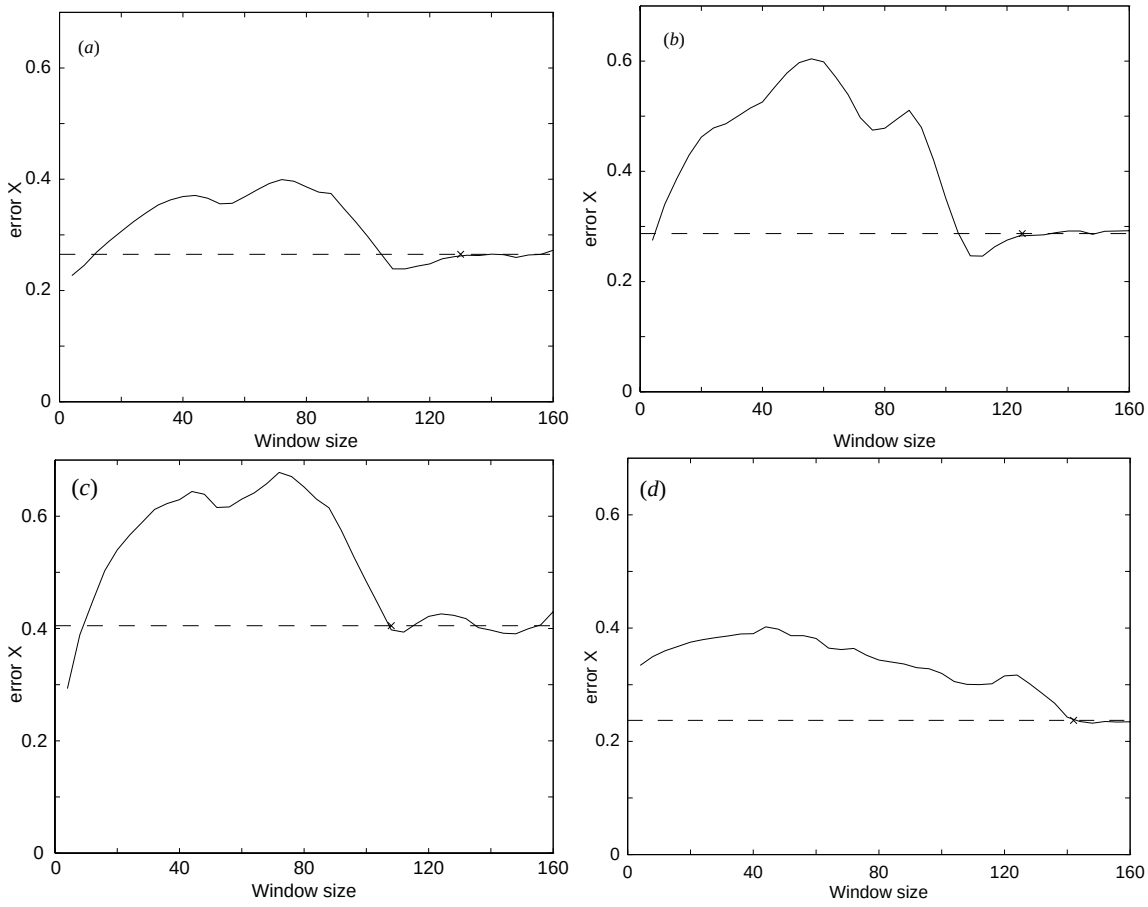


Figure 4. Fluctuation diagrams for a $192 \times 192$ plant coupled map lattice: ($a$) mixed population for $P_s = 0.7$; ($b$) mixed population for $P = 0.3$; ($c$) annual plants only ($P = 0.7$); ($d$) perennial plants only.

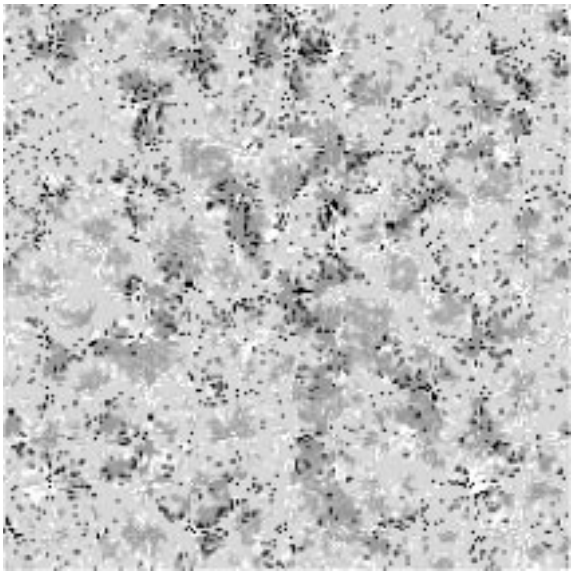

Figure 5. Example of the complex marine system: black is urchins, dark grey is microalgae, medium grey is otters, light grey is kelp and white is empty.

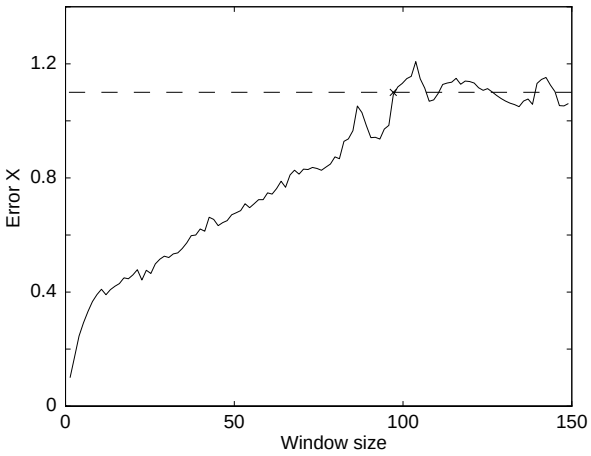


Figure 7. Fluctuation diagrams for the multispecies marine ecosystem.

This example not only demonstrates that the length scales technique agrees with our intuitions about the degree of aggregation, but that the shape of the fluctuation diagram can tell us a great deal about the spatial patterns.

### (c) *Multispecies marine ecosystem: a system with complex statistics*

In figure 5 we show a snapshot of the state of the system. The dynamics of this system are in constant flux, with the numbers of otters, urchins, kelp and algae and the statistical structure of the spatial patterns continually varying, in the sense of Appendix 1. Because of this, as discussed in § 2, in our calculation of the fluctuation at each window size we need to uti-




PHILOSOPHICAL TRANSACTIONS OF THE ROYAL SOCIETY B BIOLOGICAL SCIENCES

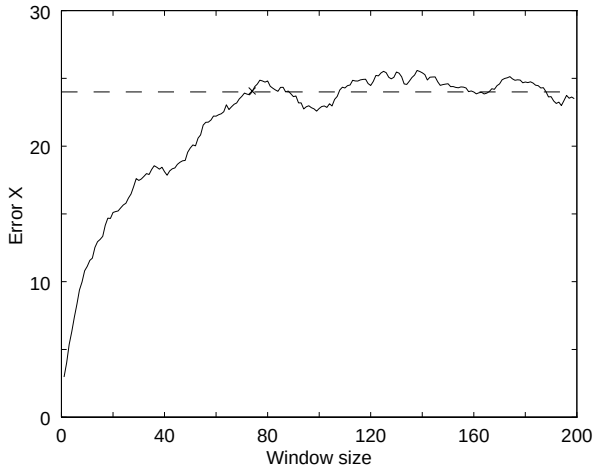


Figure 8. Fluctuation diagram for the hawk–dove system.

lize nonlinear prediction methods—the value of $A_\ell$ at the next iteration has to be predicted.

Figure 7 shows the fluctuations at window sizes from 1–150 cells; the critical length scale is around 95 cells, where the prediction error is around one percent. Figure 6*a* shows the dynamics at the coherence length $\ell_c$ by plotting the number of urchins at times $t$ and $t+30$. If the fluctuation is simply calculated with respect to the temporal mean (as for fixation systems), as opposed to the predicted value, the length scale is much larger—more than 150 cells. This is because an average over more cells is necessary to reach the limiting behaviour of random fluctuations about a mean value.

Figure 6*b* shows the first 10 eigenvalues obtained using singular value decomposition (SVD) analysis. SVD analysis gives us an independent method to check that our length scale is the size at which the deterministic portion of the dynamics is maximal compared to the noise. The results for grids of size 95 and 150 cells should be compared. It is clear that the first two eigenvalues are maximal at or close to $\ell_c$, demonstrating that at this scale the dynamics are closest to being given by a deterministic two-dimensional system. This gives the evidence that what we are observing is deterministic behaviour and that at $\ell_c$ the ratio of noise to the amplitude of the deterministic dynamics in minimized.

## 5. FLUCTUATION ANALYSIS AND MODELLING

In each of the examples considered we have identified a distinguished length scale, $\ell_c$. But, how can this observation help us when we are presented with a task of modelling a particular ecosystem? We will indicate numerically that the coherence length scale is associated with the hydrodynamic limit.

In an illuminating recent paper, Durrett & Levin (1994*b*) have described and compared different ways of modelling ecosystems. The particular system Durrett & Levin have studied is the spatially extended hawk–dove model. In this model, the interaction of two species is represented by the game matrix

| | $H$ | $D$ |
|---|---|---|
| $H$ | $a$ | $b$ |
| $D$ | $c$ | $d$ |

We shall restrict the discussion here to the interacting particle system model based on the above game matrix, with an addition of rapid diffusion at the diffusion rate $\mu$, and death due to crowding at rate $\kappa$ (for the details of this model, see Durrett & Levin (1994*b*)). In what follows, we use $a=-0.6$, $b=0.9$, $c=-0.9$, $d=0.7$, $\kappa=0.08$ and $\mu=2.0$. The fluctuation analysis for this model is given in figure 8; $X_\ell$ asymptotes to a constant at a window size of approximately 80. Durrett & Levin (1994*b*) show that, when the averaging window size $\epsilon^{-1}$ tends to infinity, and the migration rate is $\mu=4\epsilon^{-2}$, the asymptotic behaviour of the density of hawks ($u$) and doves ($v$) is governed by the following reaction–diffusion partial differential equations:

$$\frac{\partial u}{\partial t}=\Delta u + u\left[a\left(h+(1-h)\frac{u}{u+v}\right)+b(1-h)\frac{v}{u+v}\right],$$
$$\frac{\partial v}{\partial t}=\Delta v + v\left[d\left(h+(1-h)\frac{v}{u+v}\right)+c(1-h)\frac{u}{u+v}\right], \quad (3)$$

where

$$h=h(u,v)=\frac{1-\mathrm{e}^{-N(u+v)}}{N(u+v)}, \quad (4)$$

and $N$ is the number of points in the neighbourhood. The dynamical system obtained from (3) by putting the spatial derivatives to zero seems to have a globally attracting fixed point, with all of the trajectories spiralling towards that point (see figure 9*a*). Of course, if $\bar{u}$, $\bar{v}$ are the densities of hawks and doves at that fixed point, the reaction–diffusion equation (3) admits a spatially uniform steady solution given by these densities. Durrett & Levin (1994*b*) conjecture that such a solution is stable.

Note that in most real systems one cannot take the limit of the infinite system size. Thus arises the necessity of modelling at an intermediate scale characterized by $\ell_c$. For simple models, it is possible to show that, associated with finite size of the window, and in the limit where the size of the window goes to infinity, the hydrodynamic fluctuations converge to a Gaussian field (see e.g. Spohn 1991). Taking the finite window size, we expect that equations (3) need to be modified to stochastic partial differential equations where the variance of the stochastic contribution should scale as $E^u_{\ell_c}$ and $E^v_{\ell_c}$, with $E^u_{\ell_c}$, $E^v_{\ell_c}$ standard deviations for densities of hawks and doves, respectively.




PHILOSOPHICAL TRANSACTIONS OF THE ROYAL SOCIETY B BIOLOGICAL SCIENCES

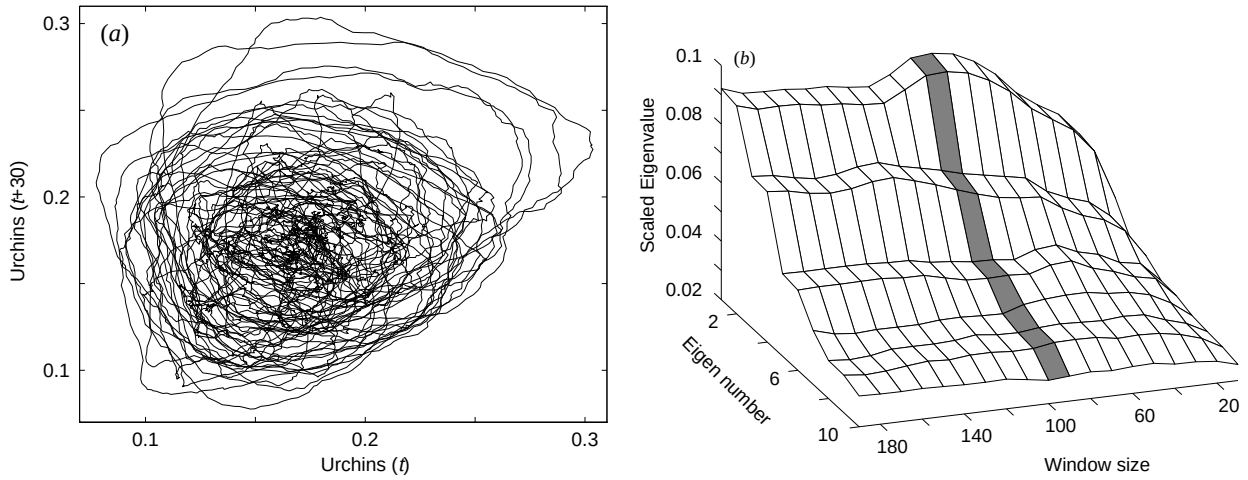


Figure 6. (*a*) The number of urchins at time $t$ against the number at time $t+30$ showing evidence of large scale cycles. (*b*) The relative magnitudes of the first 10 eigenvalues (from SVD analysis) at a range of grid sizes.

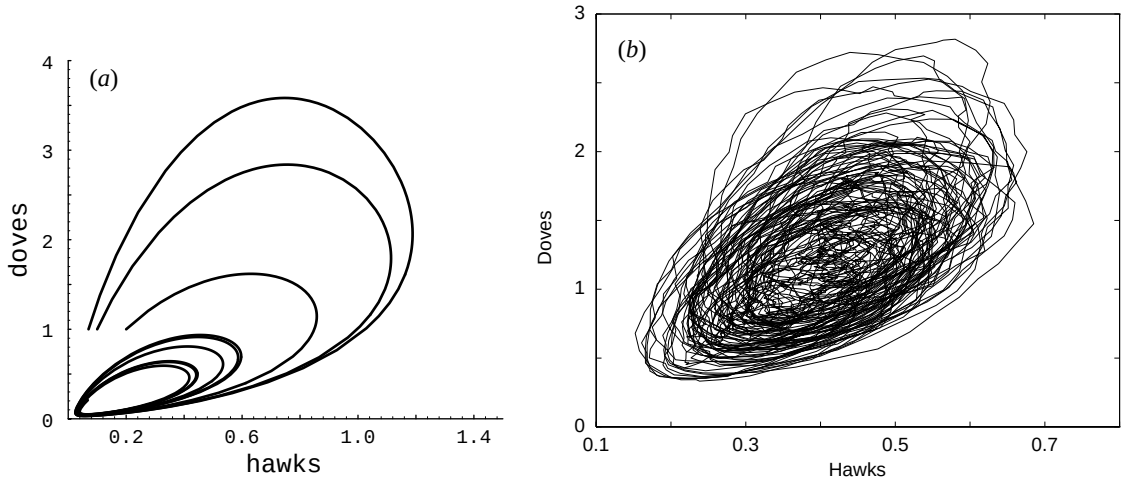


Figure 9. (*a*) Dynamics of the dynamical system associated with the partial differential equation (3). (*b*) Dynamics of the hawk–dove system from the interacting particle system averaged over a window of size 75.

In this regime, the trajectory of a stochastic system will follow the associated non-stochastic trajectory having the same initial condition. In figure 9*b* we present the result of the simulation of the interacting particle system averaged over a window of size $\ell_c$. It seems that, for this simulation, the trajectories of the dynamical system associated with (3) really serve as a 'template', so that the dynamics can be described as random jumping between its trajectories.

## 6. CONCLUSIONS

In this paper we have discussed the problem of determining the 'right' length scale for the observation of spatially extended problems in ecology. Our approach relies on averaging: we average the data obtained from the dynamics of the system over domains ('windows') of different sizes. When the window size is equal to one cell and the system is *probabilistic* or *deterministic and chaotic*, we expect the data-versus-time plot to have stochastic features. When we take the averaging window to be the whole system, and the system is large, the data-versus-time plot is a flat line (after transients). The question of whether there is a spatial scale, $\ell_c$, such that there is interesting dynamics for data averaged over a window of size $\ell_c$ was tackled in Rand & Wilson (1995). The answer depends both on the size and the nature of the system. For example, if the system has statistics that are too simple (systems with unique statistical fixation), there is no length scale that has *interesting* dynamics. But, we have shown that even in that case (and in the even simpler case of systems with fixation) interesting biological conclusions can be drawn from the *fluctuation diagram*. For example, the issues of aggregation and disaggregation have been shown to correspond to increases and decreases, respectively, in the graph of the fluctuation $X_\ell$ as a function of the window size $\ell$. When there exists a length scale with interesting dynamics, we have proposed an approach that takes account of the non-trivial deterministic dynamics. We identify the appropriate length scale by using nonlinear prediction methods for the averaged data, rather than using the global mean.

In cases, such as this, when presenting a new method for data analysis, based on assumptions about the statistical nature of the system, it is use-




PHILOSOPHICAL TRANSACTIONS OF THE ROYAL SOCIETY B BIOLOGICAL SCIENCES

ful to identify the cases in which the approach can be rigorously justified. We have pointed out that when the invariant measure of the system possesses the so-called FKG property and a fast decay of correlations, the assumption on the asymptotic behaviour of fluctuations is justified. Strictly speaking, the procedure for justifying our assumption on the scaling of the fluctuations when the size of the window is big is to establish: (1) the existence of the invariant measure to which any initial measure converges; (2) the preservation of FKG property under the dynamics (see Appendix 2); (3) the decay of correlations for the invariant measure.

To establish the preservation of FKG inequalities under the dynamics of the system is typically straightforward. On the other hand, the fast decay of correlations and the existence of the invariant measure are difficult to prove. But, the fact that the dynamics preserves FKG inequalities can serve as a sign that the scaling of the fluctuations is as required. However, the fast decay of correlations can be established numerically. For example, the dynamics of the genetic selection model preserves the FKG inequalities, and we have shown numerically that the correlations decay quickly at the asymptotic state (fixed point of the system).

It should be pointed out that the existence of $1/\ell^{d/2}$ scaling of the fluctuations for large $\ell$ is not the necessary requirement for our analysis to work. In particular, the system can exhibit the scaling of fluctuations of the $1/\ell^{\gamma}$ type, with $\gamma \neq \frac{1}{2}d$. In that case, the length scale $\ell_c$ can be identified as the scale at which the scaling regime is attained. Such a scaling is related to limiting distributions that are different from Gaussian—the so-called *stable distributions* (see e.g. Ibragimov & Linnik 1971).

We have commented in § 5 on the relationship between the hydrodynamic equations for the hawk–dove system and the dynamics on the identified coherence length scale $\ell_c$. We have shown numerically that the simulated trajectory of the system follows approximately the trajectory obtained from the hydrodynamic limit. More work is necessary to put this observation on rigorous footing. For example, the variance of the noise could be derived from the second moment of the local Poissonian distributions assumed by Durrett & Levin (1994*b*) and a stochastic partial differential equation for the evolution of the densities derived. Even then, the derivation would be heuristic, due to the complexity of the underlying mathematical apparatus, just as the original derivation in Durrett & Levin's (1994*b*) paper. To appreciate this complexity and get the information on the methods and problems arising in the derivation of the hydrodynamic limits and the analysis of stochastic partial differential equations the reader can consult Spohn (1991), De Masi & Presutti (1991), Mueller & Tribe (1994, 1995) and Tribe (1995).

The applicability of the method of fluctuation analysis to the analysis of dynamical (i.e. time varying) data obtained from remote sensing is apparent. Of course, whether interesting results are to be obtained depends on the size of the sample, as well as on the dynamics of the observables. In particular, the system size might be too small to ever achieve the required scaling limit. In that case we can say that the data has predominantly stochastic quality. On the other hand, if the size of the sample is large enough so that the limit in question is attained, the appropriate length scale can be identified and deterministic dynamics uncovered.

This work was supported by a UK Engineering and Physical Sciences Research Council studentship, a Wellcome Trust Research Training Fellowship in Mathematical Biology (M.J.K.) and the University of Warwick Graduate Department award (R.J.H.). The authors particularly wish to thank Ms R. Ball for the 'Openwindows' graphical interface for the cellular automaton and coupled map lattice programs. We are grateful to Minus van Baalen for carefully reading the manuscript and for numerous useful discussions and Roger Tribe for discussing the hydrodynamic limits and theory of interacting particle systems with us. We also thank Thomas Bohr for useful comments and Simon Levin for prompting us to discuss scalings different from the Gaussian.

## APPENDIX 1. SPATIAL STATISTICS AND INVARIANT MEASURES

Spatially extended systems defined on $\boldsymbol{Z}^d$ can exhibit a variety of asymptotic (in time) behaviour. The simplest of these is convergence to a fixed point of a system, i.e. to a configuration that is invariant under the dynamics of the system. This is an example of a deterministic asymptotic behaviour of a system. Depending on different initial conditions, a system may tend to different fixed points. Both deterministic systems (e.g. the genetic coupled map lattice that we have studied) and stochastic systems (e.g. the voter model in one dimension and the contact process) can possess such a behaviour. We call these types of models *systems with fixation*. We shall not discuss more complex asymptotically deterministic behaviour such as the limit cycles or strange attractors, as we do not analyse any systems that exhibit those.

If the rules of the process are stochastic, in the infinite time limit the motion of the system can, of course, still be stochastic. In this case, if the initial distribution $\mu$ is given, the distribution of the system may converge to an invariant measure $\nu$. Based on the properties of this invariant measure we shall distinguish between two types of systems. In particular, suppose that this invariant measure is *ergodic* with respect to the shift transformation defined by

$$\tau_i \boldsymbol{x}(j) = \boldsymbol{x}(\tau_i j) = \boldsymbol{x}(j - i),$$

where $i, j \in \boldsymbol{Z}^d$. Then we call the corresponding process a *system with statistical fixation*. Note that the shift transformation acts on functions as

$$\tau_i f(\boldsymbol{x}) = f(\tau_i \boldsymbol{x}).$$

For the definition of ergodicity of measures, see Liggett (1985).

Ergodicity of the invariant measure means that for any observable $f : \boldsymbol{Z}^d \to \boldsymbol{R}$ and almost every (i.e.

$$\frac{\partial p'_{ij}}{\partial p_{ij}} = \frac{\frac{3}{5}(A+1) + \frac{1}{5}(A+A^2)p_{ij} + (A+A^2)\Sigma_{ij} - \frac{1}{5}(A+A^2)p_{ij}^2 - (A+A^2)\Sigma_{ij}}{[2Ap_{ij}\Sigma_{ij} - A(p_{ij}+\Sigma_{ij}) + A + 1]^2} > 0,$$
$$\frac{\partial p'_{ij}}{\partial p_{kl}} = \frac{\frac{1}{10}(A+1) + \frac{1}{5}(A+A^2)p_{ij} - \frac{1}{5}(A+A^2)p_{ij}^2}{[2Ap_{ij}\Sigma_{ij} - A(p_{ij}+\Sigma_{ij}) + A + 1]^2} > 0. \tag{5}$$

except for a measure zero set in $\nu$) $\boldsymbol{x}$,

$$\lim_{i\to\infty} \frac{1}{|\{j \in \boldsymbol{Z}^d : 0 \leqslant j \leqslant i\}|} \sum_{0\leqslant j\leqslant i} \tau_j f(\boldsymbol{x}) = \int f \,\mathrm{d}\nu. \tag{6}$$

where $i = \{i_1, \ldots, i_d\}, j = \{j_1, \ldots, j_d\} \in \boldsymbol{Z}^d$, and the inequalities are to be interpreted component wise. For example, let $f(\boldsymbol{x}) = 1$ if $x_0 = 1$ and $f(\boldsymbol{x}) = 0$ if $x_0 = 0$ for a model with a state space $\{0, 1\}$. In that case, the limit (6) would give us a density of '1's for a configuration $\boldsymbol{x}$. For a system with statistical fixation, this density would be the same for almost all (with respect to the invariant measure $\nu$) configurations $\boldsymbol{x}$.

If the distribution of a system with asymptotically stochastic behaviour converges to an invariant measure $\nu$ which is non-ergodic, we call such a model a *system with complex statistical structure*.

## APPENDIX 2. FKG INEQUALITIES

We have mentioned that we can assign a number $x_i$ to each site $i$ determining the state of the system at that site (e.g. 0 = empty site, 1 = populated site). We can also order the states. For example, we can assign $0 > 1$ (note that 0 and 1 are only convenient names here, rather than numbers). In general, we might be able to assign an *order* on the state space $S$ that the $x_i$ belong to. Now we can define that a configuration $\boldsymbol{x} = \{x_i, i \in \boldsymbol{Z}^d\}$ is larger than another configuration $\boldsymbol{y} = \{y_i, i \in \boldsymbol{Z}^d\}$ if $x_i > y_i$ for every $i$. This introduces only a partial order on the space of all configurations $A$, as there are pairs of configurations that are not ordered (one configuration being bigger on some sites, the other configuration being bigger on other sites). A function $f$ on a configuration is called increasing if $\boldsymbol{x} > \boldsymbol{y}$ implies $f(\boldsymbol{x}) > f(\boldsymbol{y})$. For example, global density is an increasing function. The invariant measure $\nu$ is said to be FKG if, for any two *increasing* functions $f$ and $g$,

$$\int_A fg \,\mathrm{d}\nu \geqslant \int_A f \,\mathrm{d}\nu \int_A g \,\mathrm{d}\nu.$$

The easiest way to show that an invariant measure for a coupled map lattice or a probabilistic cellular automaton satisfies the FKG inequalities is to show that it preserves the FKG property of measures at every time step. A sufficient condition that this holds (see Mezić 1997) is the monotonicity of the system. Monotonicity means that if $f$ is an increasing function, then the expectation $(\mathbb{E})^{\boldsymbol{x}} f$ of $f$ when the system is started from a particular configuration $\boldsymbol{x}$ is an increasing function, too. In contrast with expectations from the complexity of the above definitions, the monotonicity property is checked quite easily and directly from the local rules of the system (Mezić 1997). For example, in the case of a coupled map lattice defined by

$$x_i^{n+1} = F_i(\boldsymbol{x}^n),$$

where $i$ denotes the site and $n$ the iteration, a necessary and sufficient condition for monotonicity is

$$\partial F_i / \partial x_k^n \geqslant 0,$$

for all $i$ and $k$. Analogous conditions hold for cellular automata. The first of the models studied (the genetic model) satisfies these conditions.

## APPENDIX 3. FKG INEQUALITY FOR GENETIC MODEL

The genetic model can be seen to satisfy the monotonicity condition for the FKG property to hold, see equations (5) in which $(k, l) \in \mathrm{Nhd}(i, j)$ but $(k, l) \neq (i, j)$.

## REFERENCES


Casdagli, M. 1989 Nonlinear prediction of chaotic time series. *Physica* D **35**, 335–356.

Crawley, M. J. & May, R. M. 1987 Population dynamics and plant community structure: competition between annuals and perennials. *J. Theor. Biol.* **125**, 475–489.

Czárán, T. & Bartha, S. 1992 Spatio-temporal dynamic models of plant populations and communities. *Trends Ecol. Evol.* **7**, 38–42.

DeRoos, A. M., McCauley, E. & Wilson, W. G. 1991 Mobility versus density-limited predator–prey dynamics on different spatial scales. *Proc. R. Soc. Lond.* B **246**, 117–122.

De Masi, A. & Presutti, E. *Mathematical methods for hydrodynamic limits*, Springer Lecture Notes in Mathematics 1501. New York: Springer.

Durrett, R. & Levin, S. A. 1994*a* Stochastic spatial models—a user's guide to ecological applications. *Phil. Trans. R. Soc. Lond.* B **343**, 329–350.

Durrett, R. & Levin, S. A. 1994*b* The importance of being discrete and spatial. *Theor. Popul. Biol.* **46**, 363–394.

Hassell, M. P., Comins, H. N. & May, R. M. 1991 Spatial structure and chaos in insect population dynamics. *Nature* **353**, 255–258.

Hendry, R. J. & McGlade, J. M. 1995 The role of memory in ecological systems. *Proc. R. Soc. Lond.* B **259**, 153–159.

Hendry, R. J., McGlade, J. M. & Weiner, J. 1996 A coupled map lattice model of the growth of plant monocultures. *Ecol. Model.* **84**, 81–90.

Ibragimov, I. A. & Linnik, Y. V. 1971 *Independent and stationary sequences of random variables*. Groningen: Wolters-Noordhoff.

Keeling, M. J. & Rand, D. A. 1997 Space and fluctuations in the dynamics of infection. In *From finite to infinite*

*dimensional dynamical systems* (ed. P. Glendinning). Amsterdam: Kluwer.

Keeling, M. J. 1997 Spatial models of interacting populations. In *Theoretical ecology. Advances in principles and applications* (ed. J. McGlade). London: Blackwell.

Levin, S. A. 1992 The problem of pattern and scale in ecology. *Ecology* **73**, 1943–1967.

Levin, S. A. & Durrett, R. 1996 From individuals to epidemics. *Phil. Trans. R. Soc. Lond.* B **351**, 1615–1621.

Liggett 1985 *Interacting particle systems*. Berlin: Springer.

McGlade, J. 1995 Dynamics of complex ecologies. In *Modelling the dynamics of biological systems* (ed. E. Mosekilde & O. G. Mouritsen), Springer series in Synergetics 65. Berlin: Springer.

Mezić, I. 1997 FKG inequalities in cellular automata and coupled map lattices. *Physica* D (In the press.)

Mueller, C. & Tribe, R. 1994 A phase-transition for a stochastic PDE related to the contact process. *Prob. Theory Related Fields* **100**, 131–156.

Mueller, C. & Tribe, R. 1995 Stochastic PDEs arising from the long-range contact and long-range voter processes. *Prob. Theory Related Fields* **102**, 519–545.

Newman, C. M. 1980 Normal fluctuations and the FKG inequalities. *Comm. Math. Phys.* **74**, 119–128.

Rand, D. A. 1994 Measuring and characterising spatial patterns, dynamics and chaos in spatially extended dynamical systems and ecologies. *Phil. Trans. R. Soc. Lond.* A **348**, 497–514.

Rand, D. A., Keeling, M. J. & Wilson, H. B. 1995 Invasion, stability and evolution to criticality in spatially extended artificial host–pathogen systems. *Proc. R. Soc. Lond.* B **259**, 55–63.

Rand, D. A. & Wilson H. B. 1995 Using spatio-temporal chaos and intermediate scale determinism in artificial ecologies to quantify spatially extended systems. *Proc. R. Soc. Lond.* B **259**, 111–117.

Sinai, Y. G. 1976 Self-similar probability distributions. *Theory Prob. Applic.* **21**, 64–80.

Solé, R. V. & Valls, J. 1991 Order and chaos in a 2D Lotka–Volterra coupled map lattice. *Phys. Lett.* **153A**, 330–336.

Spohn, H. 1991 *Large scale dynamics of interacting particles*. Berlin: Springer.

Tribe, R. 1995 Large time behaviour of interface solutions to the heat-equation with Fisher–Wright white noise. *Prob. Theory Related Fields* **102**, 289–311.

Weiner, J. & Conte, P. T. 1981 Dispersal and neighbourhood effects in an annual plant competition model. *Ecol. Model.* **13**, 131–147.

Wiens, J. A. 1989 Spatial scaling in ecology. *Funct. Ecol.* **3**, 385–397.

Wissel, C. 1991 A model for the mosaic-cycle concept. In *The mosaic-cycle concept of ecosystems*, Springer Ecological Studies 85 (ed. H. Remmert), pp. 22–45. Berlin: Springer.

*Received 22 October 1996; accepted 6 January 1997*



PHILOSOPHICAL TRANSACTIONS OF THE ROYAL SOCIETY B BIOLOGICAL SCIENCES

PHILOSOPHICAL TRANSACTIONS OF THE ROYAL SOCIETY B BIOLOGICAL SCIENCES